



Effect of hydrothermal temperature on synthesis of hydroxyapatite from limestone through hydrothermal method

Novesar Jamarun*, Asregi Asril, Zulhadjri, Zefri Azharman and Tika Permata Sari

Chemistry Department, Andalas University, Padang, West Sumatera, Indonesia

ABSTRACT

Nanoparticles hydroxyapatite (HAp) had been synthesized from limestone by using hydrothermal method. Precursors were limestone (CaCO_3) and diammonium hydrogen phosphate ($(\text{NH}_4)_2\text{HPO}_4$) with 1.67 ratio of Ca/P. Hydroxyapatite (HAp) was obtained by mixing precursors at pH 10 in variation temperature at 120, 160 and 200°C. The product were characterized by Fourier Transform Infrared (FTIR), X-Ray Diffraction (XRD) and Scanning Electron Microscopy (SEM). FTIR was used to determine phosphate and hydroxyl functional groups as the constituent group of hydroxyapatite. XRD data showed that all of products were hydroxyapatite. Hydroxyapatite synthesized at 200°C has smaller crystal size than others. SEM images showed that nanoparticles hydroxyapatite had spherical shape.

Keywords: Hydroxyapatite, Limestone, Hydrothermal, Nanoparticle

INTRODUCTION

Hydroxyapatites (HAp) are a calcium phosphate bio ceramic material, which has an almost identical chemical composition to mineral component of bone [1]. HAp gained considerable attraction because HAp excellent osteoconductive and osteointegration properties, allowing synthetic HAp to be used widely in clinical surgery and biomedical applications [2]. HAp are not only a biocompatible, osteoconductive, non-toxic, non-inflammatory and non-immunogenic agent, but also bioactive. HAp has ability to form a direct chemical bond with living tissues [3].

Hydroxyapatites can be produced by direct wet precipitation of calcium and phosphate ions [4]. HAp is often used in hip, knee and other implants and as a synthetic bone substitute [1]. HAp can implant in human body since they provide a good adhesion to the local tissue due to their surface chemistry and shown to enhance osteoblast proliferation [4]. HAp has also studied for other non-medical applications, for example, as packing media for column chromatography, gas sensors, and catalyst [5].

The term hydroxyapatite with a general formula is $\text{M}_{10}(\text{XO}_4)_6\text{Z}_2$, where M^{2+} is a metal and species of XO_4^{3-} and Z are anions. In hydroxyapatite, M is calcium (Ca^{2+}), X is phosphorus (P^{5+}) and Z is the hydroxyl radical (OH^-) [6]. Commercial HAp particle sizes ranged between 10-40 μm with 1.66 to 1.69 ratio of Ca/P [1]. Some studies reported that the stoichiometry of HAp plays an important role in the mechanical properties and obtaining better results when ratio Ca/P is 1.60 and 1.67 [6]. Synthetic HAp, which the chemical formula of $\text{Ca}_{10}(\text{PO}_4)_6(\text{OH})_2$, include hydroxyl groups contain impurities such as CaO, biphasic calcium phosphate (BCP, HA + β -TCP) or β -tricalcium phosphate ($\text{Ca}_3(\text{PO}_4)_2$, β -TCP) [7]. Hydroxyapatite has been synthesized with various of raw materials. The source of hydroxyapatite were derived from materials in high calcium content such as bone [3] and starch [8]. Synthesis of HAp is well known by various methods such as precipitation method [9], sol-gel [10], and hydrothermal [1].

Hydrothermal method is offer good control on morphology and chemical stoichiometric [1]. Apart of massive source of calcium ion such as limestone and hydrothermal synthesise [11], aim of the research is to synthesise

hydroxyapatite of limestone via hydrothermal method with variation of hydrothermal temperature. Some characterization (FTIR, XRD and SEM) were applied to identified the hydroxyapatite form. These characterizations aimed to determined constituent functional groups, specific surface area, particle size and morphology.

EXPERIMENTAL SECTION

Materials

Materials used in hydroxyapatite synthesis were limestone (CaCO_3), Distilled water, Nitric Acid (HNO_3), Ammonia (NH_3), Diammonium Hydrogen Phosphate ($(\text{NH}_4)_2\text{HPO}_4$). Apparatus were thermometer, glassware, magnetic stirrer, analytical balance, Whatman Filter Paper no 42, pH meters, Fourier Transform Infrared (FTIR), X-Ray Diffraction (XRD) and Scanning Electron Microscopy (SEM).

Methods

Limestone was calcined at 900°C for ± 5 hours. A total of 1.68 g sample of calcined form of CaO was dissolved in 30 mL of 2M HNO_3 through stirred for 30 minutes at 700 rpm at 65°C , and then filtered. The filtrate was titrated in 30 mL 0.6M $(\text{NH}_4)_2\text{HPO}_4$ while stirred at 700 rpm for 30 minutes with 1.67 ratio of Ca/P. pH of the solution was adjusted by NH_4OH addition to pH 10. The solution was hydrothermal treated in autoclave at 120, 160 and 200°C for 24 hours. The precipitates were dried in oven for 3 hours at 110°C . Hydroxyapatite was obtained after heating at 800°C for 5 hours. Powders characterized by FTIR, XRD and SEM

RESULTS AND DISCUSSION

Fourier Transform Infrared (FTIR) analysis

The products were analyzed by FTIR and the result are shown in Fig. 1. Spectrum FTIR of products show adsorption band at 3443, 3571, and 3572 cm^{-1} . These correspond to (OH^-) functional group. The absorptions of (PO_4^{3-}) functional group are observed at bandwidth around 962, 1019, 1062, and 1087 cm^{-1} . While the adsorption peak at 1653 cm^{-1} correspondes to (CO) functional group which indicates residual of carbonate (CO_3^{2-}). According to all of these bandwidth, the products could concluded as hydroxyapatite [5], [10].

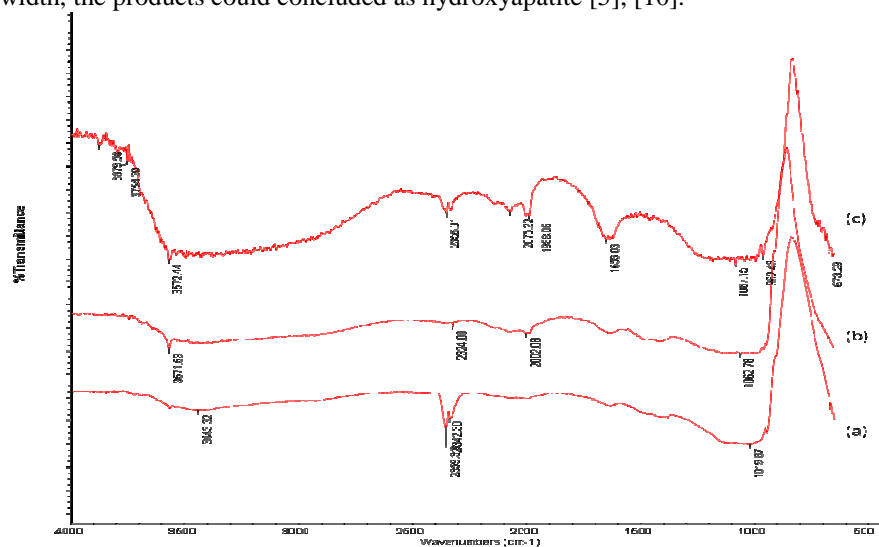


Fig 1. FTIR spectrums of hydroxyapatite synthesized by hydrothermal with variation temperatures: (a) 120°C , (b) 160°C , and (c) 200°C

X-ray Diffraction (XRD) analysis

XRD analysis used to determined whether the hydroxyapatite crystals formed as amorphous, crystalline or polycrystalline. Adsorption peaks showed structure, orientation, and crystal size. Fig. 2 showed X-Ray Diffraction pattern of hydroxyapatite at various hydrothermal temperature.

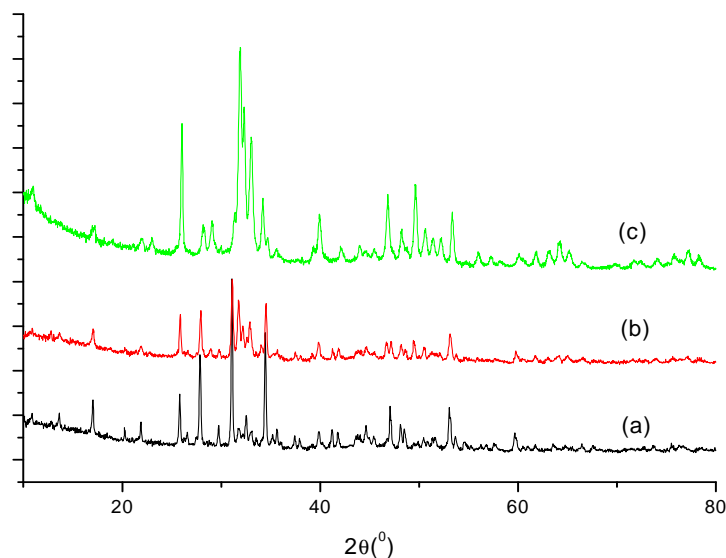


Fig 2. X-Ray diffraction pattern of hydroxyapatite at (a). 120, (b) 160, and (c). 200°C

The crystal size (D) of the sample was calculated by Scherrer equation [12].

$$D = \frac{k\lambda}{B \cos \theta}$$

Where k is Scherrer constant (k = 0.9 assuming that particles are spherical), λ is the wavelength of the incident X-rays ($\lambda = 1.54 \text{ \AA}$), β is the half width of the diffracted peak and θ is diffracted angle of values Specific surface area (S) of the HAp determined by the formula [12].

$$S = 6 \times 10^8 / d\rho$$

Where ρ is the crystallite size (nm) and d is the theoretical density of HAp (3.16 g/cm^3).

Fig. 2 showed that the sharpest peak with high intensity was at 31.0809° angle. Compound at 120°C confirmed as hydroxyapatite. The highest intensity peak at Temperature at 160°C also confirmed as hydroxyapatite. The highest intensity peak at 200°C was 31.9131° . It confirmed that the product was hydroxyapatite. XRD showed that hydroxyapatite formed at 120°C , 160°C , and 200°C had crystal phase. By using Scherrer equation, size of the HAp crystals could obtain. Size of hydroxyapatite crystals at 120°C could see in Table 1.

Table 1. Hydroxyapatite Crystal Size at 120°C

2Theta ($^\circ$)	Line width (FWHM)	Crystal Size (nm)	Specific surface area (m ² /g)
31.0809	0.1535	53.7245	35.3421
34.4373	0.1791	46.4434	40.8827
27.8659	0.1535	53.3295	35.6039

Table 1 showed that size of hydroxyapatite crystals had nanoparticle size in 46-53 nm range and specific surface area ± 35 -40 m²/g. Adsorption peaks of hydroxyapatite at 120°C showed the highest absorption intensity at $2\theta = 31^\circ$. Crystal size at 160°C can be seen in Table 2.

Table 2 Hydroxyapatite Crystal Size at 160°C

2Theta ($^\circ$)	Line width (FWHM)	Crystal Size (nm)	Specific surface area (m ² /g)
31.1244	0.2047	40.2911	47.1254
31.7926	0.2558	32.2953	58.7929
34.5162	0.1791	46.4534	40.8740

Table 2 showed that size of hydroxyapatite crystals had nanoparticle size in 32-46 nm range and specific surface area ± 40 -58 m²/g. Adsorption peaks of hydroxyapatite at 160°C showed the highest absorption intensity at $2\theta = 31^\circ$. Crystal size at 200°C can be seen in Table 3.

Table 3 Hydroxyapatite Crystal Size at 200°C

2Theta (°)	Line width (FWHM)	Crystal Size (nm)	Specific surface area (m ² /g)
26.0291	0.1574	51.8087	36.6489
31.9131	0.2362	34.9857	54.2718
32.3251	0.1378	60.0303	31.6296

Table 3 showed that size of hydroxyapatite crystals had nanoparticle size in 34-60 nm range and specific surface area \pm 31-54 m²/g. Adsorption peaks of hydroxyapatite at 200°C showed the highest absorption intensity at a $2\theta = 31^\circ$ angle. By compared the data of XRD analysis temperature at 120, 160, and 200°C, the best condition of temperature was at 200°C. Temperature at 120 and 160°C has Calcium Phosphate as impurity although hydroxyapatite has formed [10].

Scanning Electron Microscopy (SEM) analysis

SEM analysis was performed to characterize the surface morphology of the sample. In principle, surface analysis involved surface radiation with enough energy to penetrate and caused some transitions that result the emission from beam energy surface. Fig 3 showed SEM images of hydroxyapatite at 160°C.

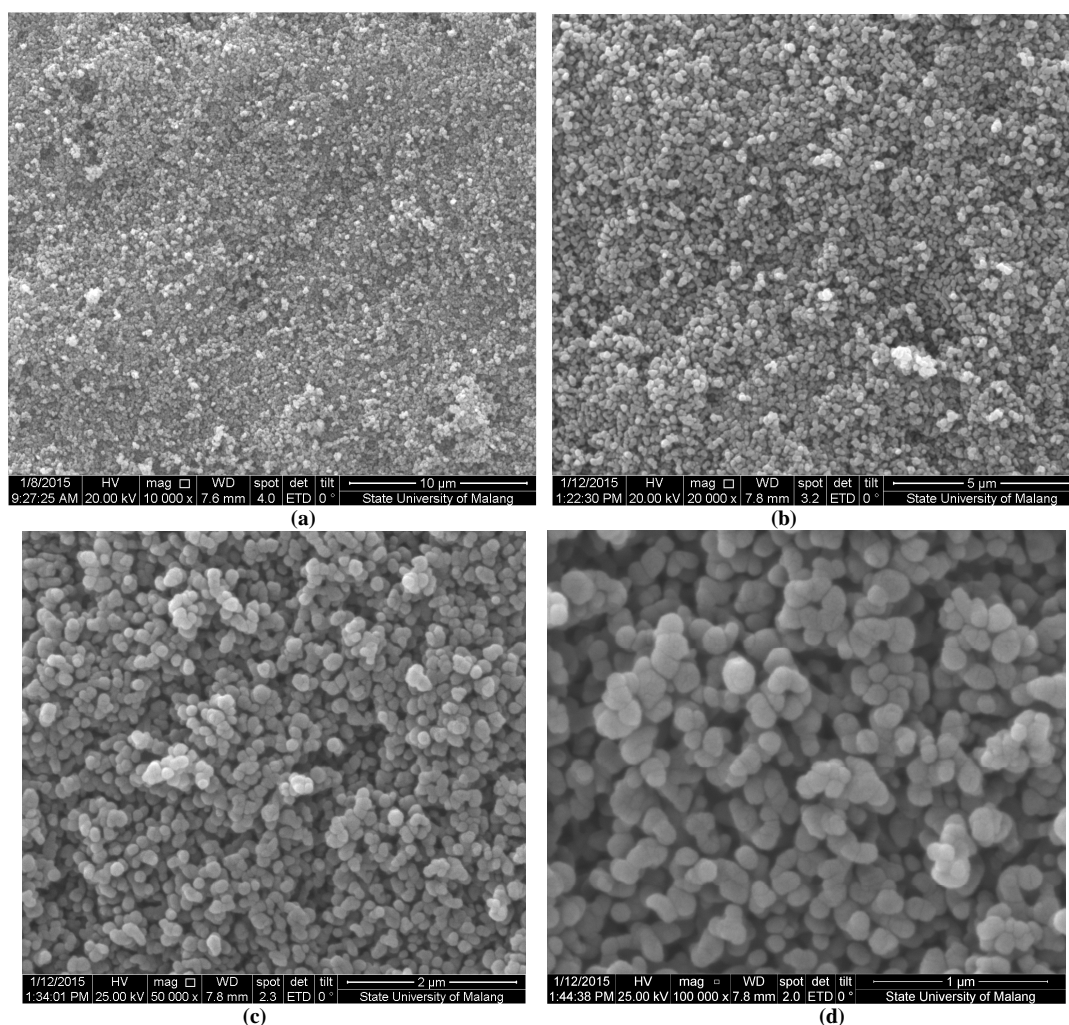


Fig 3. SEM hydroxyapatite at 160°C 10 (a) 10.000x, (b) 20.000x (c) 50.000x, (d) 100.000x

Fig. 3 showed that formation of hydroxyapatite had spherical shape. Particles of hydroxyapatite at 160°C were spread and homogeneous well without agglomeration. By using SEM-EDX, composition of hydroxyapatite compound showed by Fig 4. Table 4 showed ratio Ca/P of hydroxyapatite at 160°C was 1,293.

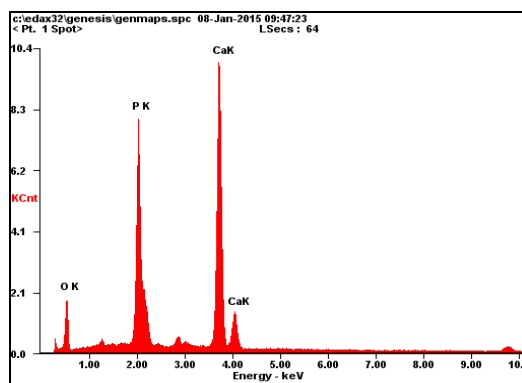


Fig 4. EDX Spectrum of hydroxyapatite at 200 °C

Table 4. Composition of Hydroxyapatite from EDX Analysis at 160 °C

Element	Wt%	At%
O K	33.08	52.97
P K	22.64	18.72
Ca K	44.29	28.31
Matrix	Correction	ZAF

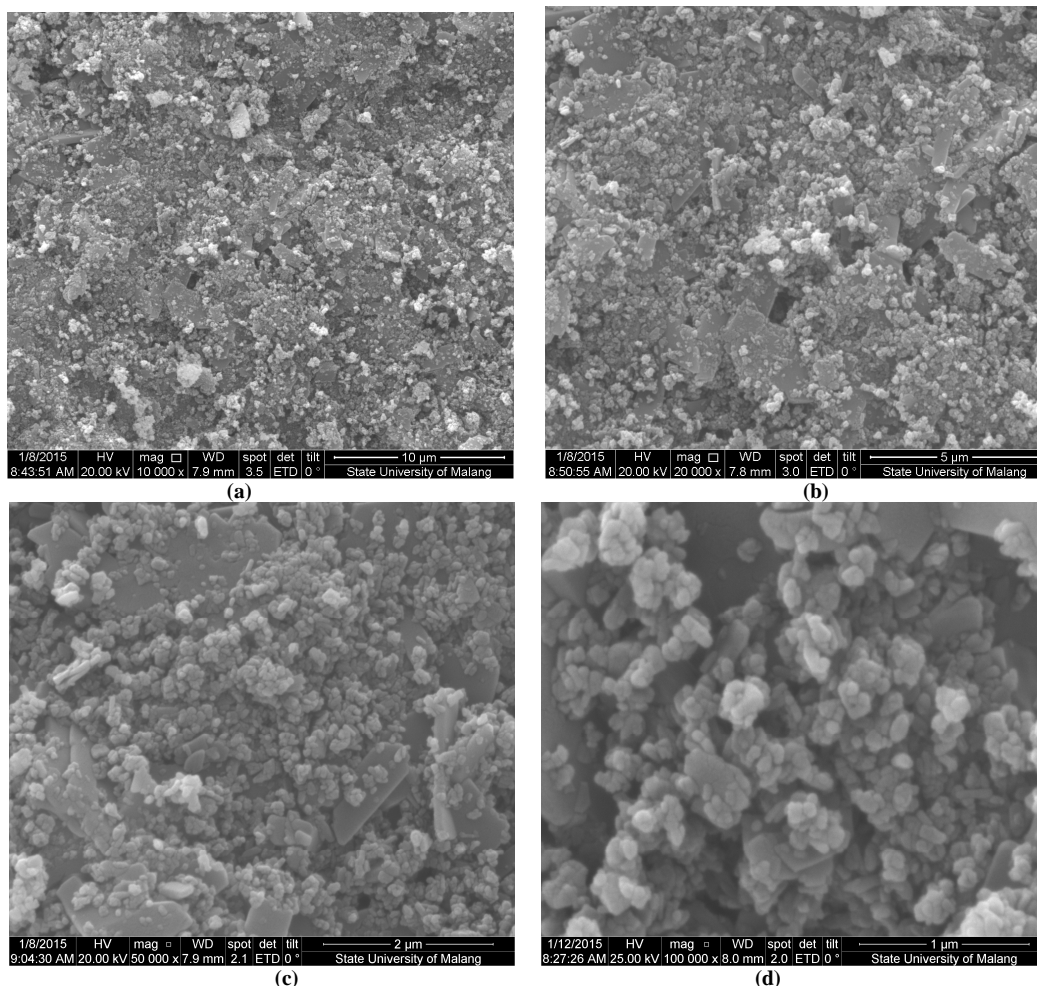


Fig 5. SEM hydroxyapatite at 200 °C 10 (a) 10.000x, (b) 20.000x (c) 50.000x, (d) 100.000x

Fig. 5 showed SEM images of hydroxyapatite at 200 °C. Fig. 5 showed hydroxyapatite had spherical shape. Particles of hydroxyapatite at 200 °C were not spread and homogeneous well. In addition, particle form of hydroxyapatite compound had agglomeration. Fig 6 showed SEM-EDX analysis of hydroxyapatite. Table 5 showed ratio Ca/P of hydroxyapatite at 200 °C was 1,296.

Table 5. Composition of Hydroxyapatite from EDX Analysis at 200°C

Element	Wt%	At%
O K	36.85	56.88
P K	23.25	18.54
Ca K	39.90	24.58
Matrix	Correction	ZAF

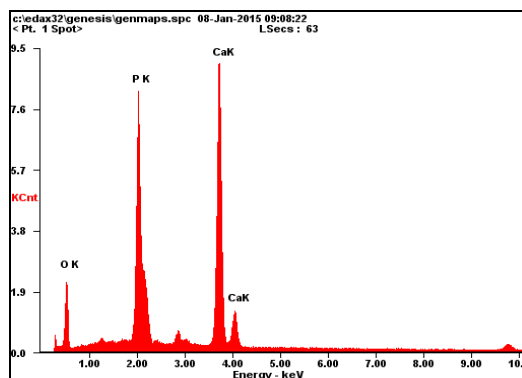


Fig 6. EDX Spectrum of hydroxyapatite at 200°C

CONCLUSION

As a result of hydrothermal method, a nanoparticle hydroxyapatite was obtained by different hydrothermal temperature. Analysis of microstructures revealed structures of hydroxyapatite. The analysis of FTIR reveals that hydroxyapatite had phosphate (PO_4^{3-}) and hydroxyl (O-H) groups although carbonate (CO_3^{2-}) group still remained. XRD revealed that size of the nanosize crystals formed and provide a large surface area. SEM images showed that hydroxyapatite had spherical shape. There are more agglomeration of hydroxyapatite particles at 200°C than hydroxyapatite particles at 160°C. The ratio of EDX analysis results in 160°C is 1,293 and in 200°C is 1.296. That is indicate that pressure and temperature influence Ca/P ratio.

Acknowledgements

The authors thanks to Ministry of Education, Republic of Indonesia, Part of this work is supported by DP2M DIKTI under Hibah kompetensi Research Grant 2015.

REFERENCES

- [1] A Dudek and L Adamczyk; *Optica Applicata.*, **2013**. 13(1) 143-151.
- [2] OR Bingöl and C Durucan; *American Journal of Biomedical Sciences.*, **2012**. 4(1). 50-59.
- [3] A Sobczak, Z Kowalski, and Z Wzorek; *Acta of Bioengineering and Biomechanics.*, **2009**. 11(4), 23-29.
- [4] DA Wahl and JT Czernuszka; *European Cells and Materials.*, **2006**. 11, 43-56.
- [5] N Jamarun; TP Sari; S Drajat; Z Azharman and A Asril; *Res. J. Pharm. Biol. Chem.Sci.*, **2015**. 6(3) 1065-1069.
- [6] R Fazel and Rezai; *Biomedical Engineering Frontiers And Challenges.*, InTech, Rijeka, **2011**. p. 374.
- [7] A Kolodziejczak-radzimska; M Samuel; D Paukszta; A Piasecki And T Jesionowski; *Physicochem. Probl. Miner. Process.*, **2014**. 50(1), 225-236.
- [8] MS Sadjadi; M Meskinfam and H Jazdarreh; *Int. J. Nano. Dim.*, **2010** 1(1), 57-63
- [9] A Singh; *Bull. Mater. Sci.*, **2012**. 35(6), 1031-1038.
- [10] TP Sari; N Jamarun; Syukri; Z Azharman and A Asril., *Oriental Journal of Chemistry*, **2014**. 30(4), 1799-1804
- [11] N Jamarun; S Yuwan; R Juita and J Rahayuningsih; *J. Appl. Chem.*, **2015**.4(2), 542-549.
- [12] M Bhagwat; P Shah and V Ramaswamy; *Materials Letters.*, **2003**. 57(9), 1604-1611.